UNPUBLISHED PRELIMINARY DATA

FINAL REPORT — NASA GRANT NsG-303

Victor Vacquier

University of California, San Diego
Marine Physical Laboratory of the
Scripps Institution of Oceanography
San Diego, California 92152

1 March 1965

Sponsored by
National Aeronautics and Space Administration
Grant NsG-303

MPL-U-2/65

FINAL REPORT — NASA GRANT NsG-303

Victor Vacquier

This grant was established to investigate the applicability of proton magnetometers to the measurement of magnetic fields on the surface of the moon from an unmanned vehicle and to explore the feasibility of measuring the magnetic properties of the moon's surface.

In the course of the investigations a study was made of the factors entering into the design of a sensing head for proton magnetometers. A summary of this study is included as Appendix I.

Some of the funds of this grant were used to assist in the construction of a portable proton magnetometer so as to provide a means for testing the differential proton magnetometer described in the proposal. This instrument has been used for archeological prospecting in California and served as the prototype of the magnetometer built for the deep towed vehicle at Scripps, the bathyscaph TRIESTE, and the magnetometer used on the GIBBS in the THRESHER search. Appendix II describes this instrument.

Although the proton magnetometer as developed has proven to be a significant contribution to geomagnetic research, the results, with respect to the purpose of the grant, have been negative. Field measurements made by space probes indicate that the magnetic field of the moon is small, probably less than 1 milligauss, making a proton magnetometer essentially unusable. The signal-to-noise ratio of this type of instrument is directly proportional to the magnitude of the ambient field. The instrument developed under this grant has a signal-to-noise ratio of 30 to 1 in the field of the Earth which is 0.5 gamma at La Jolla. It would have a signal-to-noise ratio of unity in a field of 0.17 milligauss which is likely to be the maximum value of the lunar magnetic field.

In view of the present availability of fluxgates and optically pumped magnetometers built for artificial satellites, there is no need for pursuing the development of a special proton precession magnetometer for a soft-landing vheicle. The general magnetic field of the moon is best measured by a low-altitude space vehicle rather than on the moon's surface.

Under the grant it was proposed to explore the possibility of making a thermomagnetic analysis of moon-like material with a specially constructed Curie balance. A suitable electromagnet and some quartz springs were procured; however, it became apparent that this type of balance would not be the most convenient kind for a laboratory and, in view of the progress of Project Apollo which intends to bring lunar material samples back to earth for analysis, further pursuit of the Curie balance appeared to be a waste of effort.

Dr. John Belshe and Dr. J. D. Mudie, the investigators involved in this grant, were at times working only part time for the University of California. Some of the work was done at Cambridge University, England. Then Dr. Belshe spent some time at the University of California, Los Angeles, before finally leaving for the University of Hawaii where he is employed at present. This discontinuity of residence as well as the interruption occasioned by the THRESHER disaster has considerably prolonged the work under this grant.

APPENDIX I

MPL TECHNICAL MEMORANDUM 157

AN APPRECIATION OF THE DESIGN FACTORS OF PROTON MAGNETOMETER SENSING HEADS

John D. Mudie

University of California, San Diego
Marine Physical Laboratory of the
Scripps Institution of Oceanography
San Diego, California 92152

1 March 1965

Sponsored by
National Aeronautics and Space Administration
Grant NsG-303

MPL-U-17/65

INDEX

AN APPRECIATION OF THE DESIGN FACTORS OF PROTON MAGNETOMETER SENSING HEADS

John D. Mudie

1.0 Introduction

The use of a proton magnetometer on the moon is predicated on obtaining a sufficiently strong proton signal. As the proton signal strength is proportional to the field strength, the signal-noise ratio will deteriorate in low ambient fields. A study of the factors affecting signal strength is obviously mandatory for operation on the moon.

The design of the optimum coil configuration and choice of nuclear sample are complex. and little attention has been paid to this subject in the past owing to the relative ease with which a sufficiently satisfactory detector may be designed. As the optimum design configuration varies in a complex fashion with the operational requirements, little theoretical analysis of design factors has been reported in the literature, and the design for a particular operational requirement has been arrived at on a trial and error basis.

This appreciation does not give the optimum design but discusses the various factors which influence the detection of the proton signal and discussed methods by which these factors may be evaluated.

1.1 Detector Coil Types

Three types of proton signal detection have been used:

1) Adiabatic Field Removal. In this method the polarizing field is removed slowly (i.e., in a time long compared to $2\pi/\gamma H$) either by moving the water sample out of the polarizing field (Driscoll and Bender, 1958) or by

short circuiting the polarizing field coil (Vigoureux, 1962) and then applying a short oscillating pulse of suitable amplitude and duration so that the protons are aligned normally to the over-all field.

2) Non-Adiabatic Field Removal with Separate Polarizing and Detecting Coils. This method was used in the original development of a proton magnetometer (Waters and Francis, 1958) but has since been superseded by the use of a single coil.

3) Non-Adiabatic Field Removal with a Single Coil. As will be shown later the interrelationship of the design considerations arising from the dual use of the detector cum polarizing coil are such as to render methods adopted in 1) and 2) above irrelevant. The dual use of a single coil was suggested by Waters and Francis and has since become standard in geomagnetic work.

2.0 General Analysis

This analysis follows Faini and Svelto (1962) and uses their notation. A liquid of nuclear density N (i.e., number of protons m^{-3}) consisting of molecules whose nuclei have a magnetic moment $\gamma\hbar I$ and of spin angular momentum number, I, has a nuclear paramagnetic susceptibility of

$$\chi = \frac{N\gamma^2\hbar^2 I(I+1)}{3kT} \qquad (1)$$

at an absolute temperature T (Abragam, 1961).

For protons in water at room temperature

$$\chi \approx 4 \times 10^{-9} \text{ mks.}$$

We have calculated the relative nuclear paramagnetic susceptibility of the hydrogen nuclei for a number of liquids, and these calculations appear in Table 1.

In a nuclear magnetometer the liquid sample is placed inside a coil through which a current, i_p, is passed producing a strong polarizing field $\bar{H}_p$ for a time t_p. The magnetic moments of the protons then become preferentially aligned along the resultant of the polarizing field and the earth's field, $\bar{H}_e$, generating a magnetic moment of

$$\bar{M} = \mu_o \chi(\bar{H}_p + \bar{H}_e)(1 - e^{-t_p/\tau_o}) \qquad (2)$$

TABLE 1

Name	MP°C	BP°C	Relative Proton Density
Benzene	5.51	80.093	0.609
Butyl ether	-95.2	142	0.976
Dodecane	-12	214.5	1.05
Hendecane	-26.5	195.84	1.03
Isoethyl ester	-88.2	111.7	0.809
Menthone	-6.6	207	0.942
Nonanol	-35	193	1.02
Oleic acid	+14	286	0.971
Ricinoleic acid	17	250	0.970
Ricinoleic acid, butyl ester	-	275	0.967
Tetradecene	-12	246	0.996
Tridecane	-6.2	234	1.04
Tripropylamine	-93.5	156	1.00
Pentane	-131.5	36.2	0.938
Methanol	-97.8	64.65	0.982
Water	0	100	1.0
Ethyl alcohol	-117.3	78.5	0.926
Decaline	43.26	194.6	1.05
Heptane	-90.5	98.5	0.984

where τ_0 is the longitudinal relaxation time and takes into account the energetic transitions due to thermal agitation (approximately 3 secs for pure water. $\bar{H}_p$ and therefore $\bar{M}$ vary inside the coil and may be calculated from

$$\bar{H}_p(P) = \frac{I}{4\pi} \int_{coil} \frac{I_p \bar{r} \times \bar{dl}}{r^3} \tag{3}$$

where $\bar{r}$ is the position vector of the coil segment, $\bar{dl}$, relative to the sample element under consideration at P.

The polarizing field is then removed, and the magnetization moves so that

$$\frac{d\bar{M}}{dt} = \gamma \bar{M}(t) \times (\bar{H}_p(t) + \bar{H}_e) \tag{4}$$

The motion and final orientation of the magnetization therefore depend on the manner in which the polarizing field is removed. If the polarizing field is removed sufficiently rapidly (see section on Removal of Polarizing Field), $\bar{M}$ will remain at an appreciable angle to the earth's field and precession of the protons' moments around the earth's field will occur at an angular frequency $\omega = \gamma H_e$.

The precession of the dipoles sets up a dipole moment rotating about the earth's field $\bar{H}_e$ with a magnitude of

$$\frac{\bar{M} \times \bar{H}_e}{H_e} \tag{5}$$

The rotating dipole moment may be represented by two oscillating dipoles

$$\bar{M}_1 = \frac{|\bar{M} \times \bar{H}_e|}{H_e} \sin \omega t \tag{6a}$$

$$\bar{M}_2 = \frac{|\bar{M} \times \bar{H}_e|}{H_e} \cos \omega t \tag{6b}$$

where $\bar{M}_1$, $\bar{M}_2$ and $\bar{H}_e$ are mutually perpendicular.

The oscillating dipoles generate fields of the form

$$\bar{H}_1(X) = \mu_o \iiint_{\text{sample}} \frac{[3\bar{R}\,(\bar{M}_1 \cdot \bar{R}) - \bar{M}_1]}{r^3}\, dV$$

where $r\bar{R}$ is the vectorial position of X relative to the proton sample element, dV, and $\bar{R}$ is a unit vector.

The emf generated in the coil of n turns is

$$E = -\Sigma_{\text{for each turn}} \int_{\text{over the sample}} \frac{d}{dt}\, \mu_o\, (\bar{H}_1 + \bar{H}_2) \cdot \overline{dA} \qquad (7)$$

where dA is the elemental coil area. If the coil has a series resistance R at the angular frequency ω, then the maximum signal power available is

$$W = E^2/2R \qquad (8)$$

The above equations may be used to calculate the signal produced for any given configuration of coil and sample in which a specified current is passed for a known time through the coil and is then removed in a known fashion and the signal measured with an amplifier of known noise factor. The author was unable to carry out any numerical calculations of the above equations, and the remaining rather incomplete estimations of the effects of various coil parameters on signal production have perforce been drawn from the literature.

3.0 Polarizing Time

$$W \propto (1 - e^{-t_p/\tau_o})^2 \qquad \text{ex (2)} \qquad (9)$$

and hence maximum signal is obtained when

$$t_p >> \tau_o$$

However, for a given power input the polarizing energy is proportional to time and hence the transfer efficiency (proton signal energy per unit polarizing energy),

$$\varepsilon \propto \frac{(1 - e^{-t_p/\tau_o})^2}{t_p} \tag{10}$$

The transfer efficiency obviously approaches a maximum. Hence for maximum transfer efficiency the polarizing time should be approximately $1.3\tau_o$.

3.1 Coil Sample Configuration

For a cylindrically symmetrical coil with a rectangularly shaped winding cross-section simplifications of varying degrees of accuracy may be made.

Ideal Solenoid. A solenoid of length b, of mean radius $a = \alpha b$, of winding thickness c, of number of turns N, of specific conductivity σ will be assumed to produce a uniform magnetic field $H = Ni/b$ over the sample. This magnetic field will be assumed to be normal to the earth's field. The power, P, required to produce this field is

$$i^2R = \frac{i^2N^2 2\pi a}{bc\sigma}$$

The total magnetization produced (assuming $t_p >> \tau_o$) will be

$$\chi_o H$$

If the polarizing field is removed instantaneously, the precessing magnetic moment will generate a voltage of

$$E = -\Sigma \frac{d}{dt} (\mu_o \chi_o HA) = -[\mu_o N^2 \pi (a - \frac{c}{2})^2 \chi_o i\omega f \sin\omega t]/a$$

where f is the fraction of the available sample space actually filled with sample. The maximum power delivered to the amplifier will be $E^2/2R'$, where R' is the ac resistance of the coil at the angular frequency ω.

3.2 Removal of Polarizing Field

A non-instantaneous removal of the polarizing field will result in movement of the precession axes so that the axes will not necessarily be normal to the earth's field but at an angle ϕ causing the amplitude of the signal to be

only cosø of that expected for $\phi = \pi/2$. The critical portion of the polarizing field removal is when the polarizing field becomes comparable with the earth's field (Waters and Francis, 1958), and the criteria for rapid removal is that

$$\frac{di_p}{dt} \ll \gamma H_e^2$$

This condition will be satisfied by the circuit in Fig. 1 in which the components are chosen so that the voltage across the bottle during removal of the polarizing field is such that

$$V = L\frac{di}{dt}$$

$$= \frac{Lb}{N}\frac{dH}{dt}$$

$$\gg \frac{Lb}{N}\gamma H_e^2$$

In addition the coil cable circuit must have a natural resonant frequency greater than 8 kcs (Bullard, Mason, and Mudie, 1964).

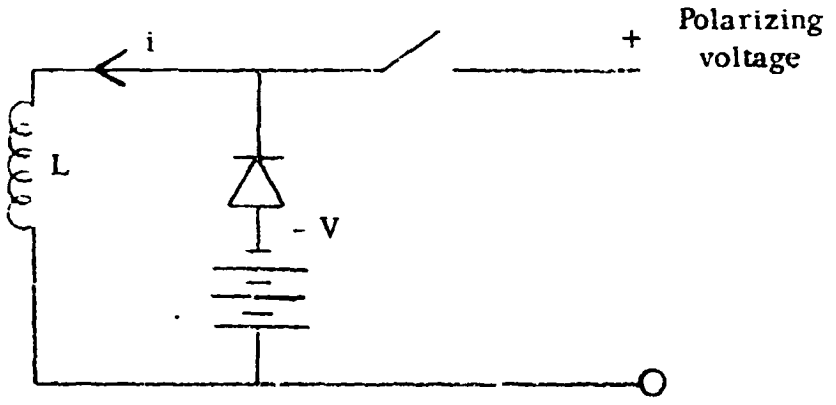

Fig. 1. Circuit for Rapid Removal of Polarizing Field

3.3 Amplifier and Tuned Circuits

The noise power in a bandwidth B from the coil is

$$E_N^2/R = 4\,kTB$$

and thus the signal-noise power ratio will be

$$S_N^2 = V^2/E_N^2$$

If $S_N >> 1$ the noise will introduce a mean squared timing error of

$$\Delta t^2 = 1/\omega^2 S_N^2$$

which will result in a relative rms scatter of $\Delta t/T$ where T is the measurement period and S_N the signal-noise ratio at the end of the period of measurement. (Strictly the scatter at the beginning of the interval of measurement should also be allowed for; this will increase the rms scatter factor by $\sqrt{1 + e^{-2T/\tau}}$.)

3.4 Other Considerations

Non-Ideal Solenoidal Coil. The polarizing field inside a solenoid of finite length varies both axially and radially. In addition the rotation magnetization is not perfectly linked to the coil. An analysis has been made by Faini and Svelto (1962) for single-layer coils, and their results may be used to calculate the over-all coupling factor for each layer of the coil. An average coupling factor for a multi-layer coil may be found by weighting the coupling factor of each layer by the fractional volume of the sample occupying the coil area. For a coil of mean radius half the length, the coupling factor $\eta(\alpha) = 0.5$.

Winding Space Utilization. As the winding space of the coil is not completely utilized, the resistance of the coil is increased to WR where W is the fractional cross-sectional area of the winding space utilized by the conducting material.

Skin and Proximity Losses. Although the skin depth at 2000 c/s is 5 cm in copper, skin-effect eddy and proximity losses are appreciable in

multi-layer coils. For the coil constructed by Faini and Svelto the ac resistance of the coil is 1.5 times the low frequency resistance resulting in a power loss of 30 per cent.

Terman (1943) gives a number of equations which enable the ac resistance of a coil to be calculated.

Amplifier Noise. As any practical amplifier will introduce noise, the signal-noise-power ratio as observed at the output of the amplifier will be reduced by a factor N' where N' is the noise factor of the amplifier.

Radiation Damping. The electrical energy accompanying the generation of the signal voltage and associated signal current flowing in the input circuit is abstracted from the precessional energy of the protons and could lead to a rapid decay of the proton signal. Bloemberger and Pound (1954), neglecting the intrinsic relaxation, state that the signal strength should decay according to

$$E_s = E_{so} \operatorname{sech} \frac{t}{\tau_1}$$

where $\tau_1 = 1/(4\pi\gamma\chi_o H_P Q^* \eta)$ and Q^* is the working Q of the coil provided that the proton magnetization is originally at right angles to the earth's field.

For a polarizing field of 100 oersteds

$$\tau_1 = 200/Q^*\eta$$

and thus radiation damping for water ($T_1 \approx 3$ secs) is appreciable when

$$Q^*\eta \geq 30$$

Power Dissipation. For operations in which the measurements are made frequently over a long period of time, consideration must be given to the temperature rise of the coil.

If ΔT is the allowable temperature difference between the coil surface and the surrounding medium, then

$$R_1^2 \leq 2\pi\left(a + \frac{c}{2}\right) bh\Delta T$$

where h is the heat transfer coefficient. This is true provided that $Kc \ll h$

where K is the thermal conductivity of copper (i.e., provided that there is a negligible temperature difference between the inner and outer layers of the coil).

4.0 Experimental Measurements

Six different coil sample configurations were constructed and connected to the input of the portable proton magnetometer (Mudie and Belshé, 1965). The coil was matched into the amplifier using the formula given in Mudie and Belshé (1965) and tuned to resonance at the proton frequency. Polarizing voltage was then applied and the polarizing current measured. The polarizing current and coil resistance were used to calculate the polarizing power, P, dissipated in the bottle. The polarizing field was then removed, and the peak signal amplitude, S, out of the portable proton magnetometer was monitored on an oscilloscope screen and photographed. An arbitrary figure of merit, S^2/P, and the decay constant for each bottle were measured and are given in Table 2. A "typical" photograph appears in Fig. 2.

5.0 Conclusions

The observed figures of merit vary by a factor of 200 depending on the design of the bottles. As the bottles differ from each other in more than one parameter, it is not easy to separate the influences of the various parameters. These measurements were originally made to provide an experimental check on calculations based on the theoretical considerations.

Acknowledgments

The author wishes to acknowledge the initiation of the analysis and the interest shown in it by Dr. J. C. Belshé, and to thank D. Leitner for calculating Table 1, G. Forbes for constructing the experimental coils, and J. Henthorn for assistance in the measurements.

Bottle No.	Length cm	Coil I.D. cm	Coil O.D. cm	Wire Diameter cm	Inductance L mH	Resistance Ω	$Q_{meas.}$ 1000 Hz Q	Polarizing Power W^P	Proton Signal S volts	S^2/P	τ secs
5	13.0	7.6	8.2	.138	13.40	2.82	16.7	34.6	2.6	.185	1.24
								16.1	1.68	.178	1.21
								4.0	1.04	.27	1.15
6	10.2	4.4	6.16	.1111	73.03	12.03	33.9	23.6	5.66	1.36	1.35
								5.91	2.15	.78	1.38
								1.48	1.40	1.32	1.8
7	5.08	4.70	*NM	.0711	54.81	7.08	39.7	39.5	2.79	.197	1.85
								9.85	1.2	.146	2.5
								2.477	.58	.137	2.43
8	10.8	6.03	10.8	.087	448.3	29.49	69	12.4	.4	.013	
9	7.94	6.03	9.55	.087	167.3	15.75	52	21.2	2.60	.312	.68
								5.28	1.25	.273	.76
								1.32	.77	.45	.69
10	10.8	6.03	8.25	.087	85.2	12.01	40	25.4	10.0	3.96	1.4
								6.25	4.0	2.57	1.5
								1.56	1.7	1.85	1.75

* Not measurable as coil had been potted. Number of turns = 1250.

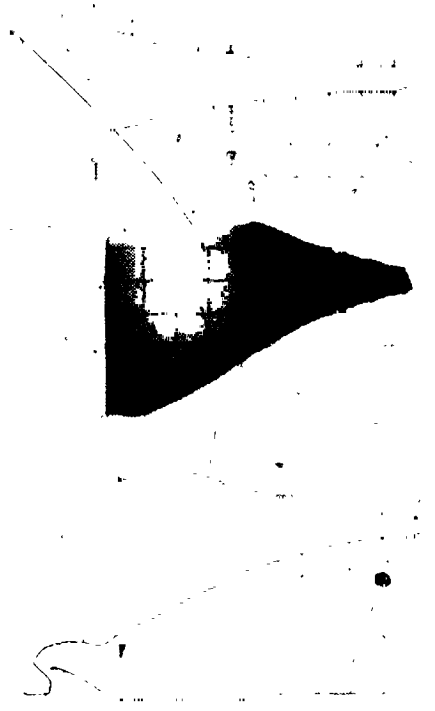

Upper Trace	Bottle #7	Polarizing Voltage	20 V
Middle Trace	Bottle #10	Polarizing Voltage	20 V
Lower Trace	Bottle #10	Polarizing Voltage	10 V
Scale	500 msecs cm^{-1}		1.0 volts cm^{-1}

Fig. 2. Typical Photograph of Proton Signal

REFERENCES

Abragam, A. (1962): The Principles of Nuclear Magnetism, Oxford University Press.

Bloemberger, N. and R. V. Pound (1954): Phys. Rev., 95, 1, 8.

Bullard, E. C., C. S. Mason and J. D. Mudie (1964): Proc. Cambridge Phil. Soc., 60, 287-293.

Driscoll, R. L. and P. L. Bender (1958): Phys. Rev. Letters, 1, 413.

Faini, G. and O. Svelto (1962): Supp. Del Nuovo Cimento, V. 23, X, 55-65.

Hall, E. T. (1963): Archaeometry, 5, 139-145.

Mudie, J. D. and J. C. Belshé (1965): Portable Proton Magnetometer, MPL Technical Memorandum No. 156.

Terman, F. E. (1943): Radio Engineers Handbook, McGraw-Hill, New York.

Vigoureux, P. (1962): Proc. Roy. Soc. A, 270, 72.

Waters, G. S. and P. D. Francis (1958): J. Sci. Instr., 35, 88.

APPENDIX II

MPL TECHNICAL MEMORANDUM 156

PORTABLE PROTON MAGNETOMETER

John D. Mudie and John C. Belshé

University of California, San Diego
Marine Physical Laboratory of the
Scripps Institution of Oceanography
San Diego, California 92152

1 March 1965

Sponsored by
National Aeronautics and Space Administration
Grant NsG-303

MPL-U-35/63

INDEX

PORTABLE PROTON MAGNETOMETER

John D. Mudie and John C. Belshé*

1.0 Introduction

Knowledge of the spatial and temporal variations of the earth's magnetic field may be useful in analyses of the main magnetic field, for elucidating the structure and magnetic properties of the earth's crust or its soils, and in studying the interaction of the solar stream upon the exosphere of the earth. Since their introduction in the early 1950's nuclear magnetometers have been successfully used in all such applications. The portable proton magnetometer described in this report measures the total geomagnetic field intensity to an accuracy of one gamma ($1\ \gamma = 1 \times 10^{-5}$ oersted) with a minimum time between measurements of six seconds.

Nuclear magnetometers were introduced into marine survey work at the Scripps Institution of Oceanography in 1958 and soon supplanted the fluxgate magnetometers which had been used there previously. These nuclear magnetometers are of the free nuclear precession type and are described by Warren and Vacquier (1961).

During Expedition Monsoon (1959-60) a desire arose for a portable version of the proton magnetometer which would permit rapid magnetic surveys on oceanic islands. One of the authors (JCB) began designing such a unit at that time following closely the circuit specifications he had given an Oxford University laboratory in 1957 to construct an instrument for surveying sites scheduled for archeological investigation. An instrument has been subsequently developed to a commercial form by the Littlemore Engineering Company of Oxford, (Aitken, 1961) and similar ones were constructed by Dr. Fred Gray of Imperial College, London, and Dr. I. Scollar of the Rheinisches Landes Museum, Bonn. All these designs followed the method of measurement suggested by Waters and Francis (1958). A portable transistorized magnetometer was designed and constructed in 1962 (JDM) following the Waters and Francis method. Provisions were made in the original design to permit easy adaptation of the portable device to marine use, as discussed in section 5.

---

* Current address Institute of Geophysics, University of Hawaii, Honolulu.

2.0 Principle of a Nuclear Magnetometer

The first experimental determination of the magnitude of the earth's magnetic field by measurement of the precession frequency of protons was carried out by Packard and Varian (1954) following a suggestion by Bloch (1946). Development of the method was subsequently carried out by Waters and Francis (1958) who measured the earth's magnetic field as follows.

Partial alignment of the protons was produced by a strong polarizing field approximately normal to the earth's field; the polarizing field was removed quickly and a measurement made of the frequency of precession of the protons about the earth's field. In order to obtain an accuracy of 1 gamma, the technique adopted was to measure the time, T, taken for a fixed number of proton precessions (usually about 2000) to occur. This was determined by counting the number of pulses generated from a standard crystal clock (100 kHz) during the time interval T.

Other absolute proton magnetometers have been devised which were based on different principles, for example:

a) that of Warren and Vacquier (1961) who formed the fourth harmonic of the proton frequency and determined the number of cycles occurring in a fixed time;

b) that of Varian Associates who determined the beat note with a fixed oscillator by using resonant reeds (Varian Associates). However these methods are less precise than that of Waters and Francis and their method of measurement was therefore adopted.

2.1 Proton Motion

The nucleus of an atom has an intrinsic spin momentum $\hbar\bar{I}$ and an associated co-linear magnetic dipole moment $\gamma\hbar\bar{I}$ where γ is the nuclear gyromagnetic ratio. For hydrogen, $I = \pm 1/2$, and for protons in water $\gamma = 2 \cdot 67513 \cdot 10^4 \times 1$ oersteds^{-1} sec^{-1} (Vigoureux, 1963).

The equation of motion of the angular momentum operator in the Heisenberg system of matrix mechanics (following Abragam, 1961) is

$$\frac{\hbar}{i}\frac{d\bar{I}}{dt} = \left[\mathcal{H}, \bar{I}\right]$$

where $\mathcal{H} = -\gamma\hbar(\bar{H} \cdot \bar{I})$ is the Hamiltonian describing the coupling of the spin with the magnetic field H;

$$\therefore \frac{\hbar}{i} \frac{d\bar{I}}{dt} = \left[-\hbar\gamma\bar{H} \cdot \bar{I}, \bar{I} \right].$$

Consider the z component,

$$\frac{\hbar}{i} \frac{dI_z}{dt} = \gamma\hbar \{ H_x \left[I_x, I_z \right] + H_y \left[I_y, I_z \right] + H_z \left[I_z, I_z \right] \}.$$

Now by elementary quantum theory (Schiff, p. 142),

$$\left[I_x, I_z \right] = i\hbar I_y, \left[I_y, I_z \right] = -i\hbar I_x \text{ and } \left[I_z, I_z \right] = 0.$$

Hence

$$\frac{\hbar}{i} \frac{dI_z}{dt} = \frac{\gamma\hbar}{i} \{ I_x H_y - I_y H_x \},$$

i.e.,

$$\frac{dI_z}{dt} = \gamma \left[\bar{I} \times \bar{H} \right]_z.$$

Classical theory predicts that a magnetic dipole strength $\bar{M} = \gamma \bar{I}$ associated with an angular momentum $\bar{I}$ in a magnetic field $\bar{H}$ will move so that

$$\frac{d\bar{I}}{dt} = \bar{M} \times \bar{H} = \gamma \bar{I} \times \bar{H},$$

i.e., the expectation value of $\bar{I}$ taken over the wave function of a free spin $\bar{I}$ obeys the same equation as the classical case and hence the classical approach is valid provided we are dealing with large number of identical non-interacting spins. The large number of quanta of angular momentum contributing to the total allows the angular momentum to be treated classically; quantization of the individual angular momenta will not be noticeable in the over-all total.

Spin interactions, which are not negligible, cause the addition of three further terms to the equation of motion, viz.

$$\frac{d\bar{M}}{dt} = \gamma \bar{M} \times \bar{H} - \frac{(\bar{M} \cdot \bar{i})\bar{i}}{T_2} - \frac{(\bar{M} \cdot \bar{j})\bar{j}}{T_2} - \frac{\{ (\bar{M} - \bar{M}_o) \bar{k} \} \bar{k}}{T_1}$$

where $\bar{k}$ is a unit vector along $\bar{H}$ (Bloch, 1946). The extra terms govern the rate of approach to equilibrium conditions. T_1, the longitudinal relaxation time, is a measure of the time interval between nuclear collisions, and T_2, the traverse relaxation time, arises from inhomogeneities in the magnetic field at the nuclei due to

a) the magnetic fields caused by other nuclei, and
b) the inhomogeneity of the over-all magnetic field.

For a liquid of low viscosity, a) is averaged out by the thermal motion of the molecules. For protons in water in a homogeneous magnetic field, the over-all relaxation time $\tau = T_1 = T_2 = 2.5$ secs. The equilibrium magnetization $\bar{M}_o$ for protons in a field H is

$$\bar{M}_o = \frac{n\gamma^2\hbar^2\bar{H}}{2kT}$$

$$= \chi \bar{H}$$

where χ is the static nuclear susceptibility (Abragam, 1961); for water at room temperature, $\chi = 3 \times 10^{-10}$ cgs units. The additional terms cause the precessing protons to lose coherence and the signal amplitude (section 2.2) thus decays exponentially with a time constant of about 2.5 secs in a homogeneous field. Note that a magnetic field gradient of 2γ cm^{-1} or greater will also cause a more rapid signal decay due to variations in precessional frequency across the sensing head (bottle).

2.2 Production of Proton Signal

In a proton magnetometer a large polarizing field, c. 100 oersteds, is applied at right angles to the earth's field for a period comparable to τ. At the end of the polarizing period, if the magnetization acquired before polarization is neglected, the protons are preferentially aligned along $(\bar{H}_p + \bar{H}_e)$ and $\bar{M} \times (\bar{H}_p + \bar{H}_e)$ is zero. If the polarizing field is removed instantaneously, the couple $\bar{M} \times \bar{H}_e$ acting on the protons causes the spin axis to precess about the earth's field at the Lamor frequency ω such that

$$\bar{\omega} \times \bar{I} = \bar{M} \times \bar{H}$$

so that

$$\omega = -\gamma H.$$

The rotating magnetic field caused by the dipole precession induces a voltage in the polarizing coil which is then amplified. The amplitude of the rotating field is $\frac{\chi \bar{H}_p \times \bar{H}_e}{H_e}$ and generates a voltage of the order of microvolts in the coil. The signal has a frequency of 2000 Hz for an ambient field of 0.5 oersteds. The signal is amplified in a narrow bandwidth high-gain audio amplifier and T (the time taken for 1000 precession cycles to occur) measured. During T, pulses from a standard 100 kHz crystal oscillator are counted in a set of five decade counters and thus the field H (in oersted) may be determined.

$$H = \frac{2\pi f}{\gamma}$$

$$= \frac{2\pi}{\gamma} \quad \frac{1000}{T}$$

$$= \frac{2\pi}{\gamma} \quad \frac{1000 \times 10^5}{C} \text{ oersteds}$$

where $\gamma = 2 \cdot 67513 \times 10^4 \text{ oersteds}^{-1} \text{ sec}^{-1}$ and C is the decade count as indicated on the front panel meters. A set of tables relating H and C appear in section 3.3

3.0 Operating Instructions

3.1 Adjustments

1. Set timing controls BT1, BT2, CT1, CT2 and CT3, to suitable values using Figs. 1 and 2 or 3.

2. Connect supplies, C, -24 volts or -12 volts; A, -12 volts (may be parallel with C); F common + ve ground on BATTERY plug; connect detector to BOTTLE socket and set detector approximately E - W.

3. Switch On; set FUNCtion switch to INDicate.

4. Press "set 0" button. All meters should read 0. If not adjust as detailed in section 4.5b of this manual

5. Press "set 9" button. Rotate "adjust 9" control to set all meters at 9. If they cannot all be set to read 9 simultaneously, adjust as detailed in section 4.5b of this manual.

6. Set FUNCtion switch to MONitor and press POLARIZE button.

7. After 4 secs meter will flick; observe the maximum reading. Adjust bottle and tuning controls for maximum signal amplitude (usually about 6) by pressing POLARIZE button and observing variation of signal amplitude with tuning setting.

8. Set FUNCtion switch to INDicate and observe count. The count may be converted to field strength by use of tables in section 3.3.

9. For valid readings, the detector should be at least 5 meters from the instrument; in addition the detector, cable and tuning controls should not be disturbed during the counting period.

3.2 Circuit Functions

A measurement is initiated by pressing the POLARIZE button which triggers a timer unit (DT1, see Fig. 4). The timer unit, via the relay control unit (S4a), energizes the polarizing relays A and B in the preamplifier (Fig. 5). These relays apply a polarizing voltage to the detector coil and also reset the counters and control circuits. After 4 secs the timer reverts to its quiescent state and the polarizing relays are released removing the polarizing field. The detector bottle is then connected to the amplifier. The bottle coil is tuned to the proton frequency by the "bottle tuning" capacitors BT1 and BT2. The signal is amplified in a 3-stage low-noise transistor amplifier in S1 and fed (via a link S to B on plug P2) to a high Q filter (Fig. 6) tuned by CT1, CT2 and CT3 to the proton frequency (tuning settings for various field values appear in Figs. 1 and 2 and for various locations in Fig. 3).

After filtering, the signal is further amplified in S2 and fed to the pulse shaper PS1 which produces sharp pulses suitable for the counting circuits. A special circuit (S3 and S4b, Fig. 4) indicates the signal amplitude on meter 1 when the FUNCtion switch is set to the MONitor position. The divide chain A_3, A_2 and A_1 produces a single pulse for each 1000 proton pulses and these are fed to an interlocked binary control, B_1 and B_2, which opens the gate G_1 for the duration of 1000 proton pulses. During this time 100 kHz pulses from the crystal oscillator, OSC, are transmitted through the gate and are counted in the decade dividers, C5, C4, C3, C2, and C1, the counts of which appear on the meters on the front panel.

Table 3.3 Field in Oersted vs Count

	.0	100.0	200.0	300.0	400.0	500.0	600.0	700.0	800.0	900.0
20000.0	1.17437	6853	6274	5701	5134	4573	4017	3466	2920	2380
21000.0	1.11845	315	790	269	9754	9244	8738	8237	7740	7248
22000.0	1.06761	278	5799	5325	4854	4388	3927	3469	3015	2565
23000.0	1.02119	1677	1239	804	374	9946	9523	9103	8687	8274
24000.0	.97864	458	55	6656	6260	5867	5477	5091	4707	4327
25000.0	.93950	575	204	2836	2470	2107	1748	1391	1036	685
26000.0	.90336	9990	9647	9306	8967	8632	8299	7968	7640	7314
27000.0	.86990	669	351	34	5720	5409	5099	4792	4487	4184
28000.0	.83884	585	289	2994	2702	2412	2124	1838	1553	1271
29000.0	.80991	713	436	162	9889	9618	9349	9082	8817	8553
30000.0	.78291	31	7773	7516	7261	7008	6756	6506	6258	6011
31000.0	.75766	522	280	40	4801	4563	4327	4093	3860	3628
32000.0	.73398	169	2942	2716	2492	2269	2047	1827	1608	1390
33000.0	.71174	959	745	533	322	112	9903	9696	9489	9284
34000.0	.69081	8878	8677	8476	8277	8079	7883	7687	7493	7299
35000.0	.67107	6916	6726	6537	6349	6162	5976	5791	5607	5425
36000.0	.65243	62	4882	4704	4526	4349	4173	3998	3824	3651
37000.0	.63479	308	138	2969	2801	2633	2466	2301	2136	1972
38000.0	.61809	647	485	325	165	6	848	691	535	379
39000.0	.60224	70	9917	9764	9613	9462	9312	9162	9014	8866
40000.0	.58719	572	426	281	137	7994	7851	7709	7567	7426
41000.0	.57286	147	8	6870	6733	6596	6460	6325	6190	6056
42000.0	.55922	790	657	526	395	264	135	6	4877	4749
43000.0	.54622	495	369	243	118	3994	3870	3747	3624	3502
44000.0	.53380	259	139	19	2900	2781	2662	2545	2427	2310
45000.0	.52194	78	1963	1849	1734	1621	1507	1395	1283	1171
46000.0	.51060	949	839	729	619	511	402	294	187	80
47000.0	.49973	867	761	656	551	447	343	240	137	34
48000.0	.48932	830	729	628	528	428	328	229	130	31
49000.0	.47933	836	739	642	545	449	354	258	163	69
50000.0	.46975	881	788	695	602	510	418	326	235	144
51000.0	.46054	5964	5874	5784	5695	5607	5518	5430	5342	5255
52000.0	.45168	81	4995	4909	4823	4738	4653	4568	4484	4400
53000.0	.44316	232	149	66	3984	3902	3820	3738	3657	3576
54000.0	.43495	415	335	255	175	96	17	2939	2860	2782

Table 3.3 (Cont'd)

	.0	100.0	200.0	300.0	400.0	500.0	600.0	700.0	800.0	900.0
55000.0	.42704	627	550	473	396	320	244	168	92	17
56000.0	.41942	867	793	718	644	571	497	424	351	278
57000.0	.41206	134	62	990	919	848	777	706	636	565
58000.0	.40496	426	356	287	218	149	81	13	9945	9877
59000.0	.39809	742	675	608	541	475	408	342	277	211
60000.0	.39146	81	16	8951	8886	8822	8758	8694	8631	8567
61000.0	.38504	441	378	316	253	191	129	67	6	7944
62000.0	.37883	822	761	700	640	580	520	460	400	341
63000.0	.37282	223	164	105	46	6988	6930	6872	6814	6756
64000.0	.36699	642	585	528	471	415	358	302	246	190
65000.0	.36134	79	24	5968	5913	5859	5804	5749	5695	5641
66000.0	.35587	533	479	426	373	319	266	213	161	108
67000.0	.35056	4	4951	4900	4848	4796	4745	4693	4642	4591
68000.0	.34540	490	439	389	338	288	238	189	139	89
69000.0	.34040	3990	3941	3892	3844	3795	3746	3698	3650	3601
70000.0	.33553	506	458	410	363	315	268	221	174	128
71000.0	.33081	34	2988	2942	2896	2850	2804	2758	2712	2667
72000.0	.32621	576	531	486	441	396	352	307	263	219
73000.0	.32175	131	87	43	1999	1956	1912	1869	1826	1783
74000.0	.31740	697	654	612	569	527	484	442	400	358
75000.0	.31317	275	233	192	150	109	68	27	986	945
76000.0	.30904	864	823	783	743	702	662	622	583	543
77000.0	.30503	464	424	385	345	306	267	228	189	151
78000.0	.30112	73	35	9997	9958	9920	9882	9844	9806	9769
79000.0	.29731	693	656	618	581	544	507	470	433	396
80000.0	.29359	323	286	250	213	177	141	105	69	33
81000.0	.28997	961	925	890	854	819	784	748	713	678
82000.0	.28643	608	573	539	504	470	435	401	366	332
83000.0	.28298	264	230	196	162	129	95	61	28	7995
84000.0	.27961	928	895	862	829	796	763	730	697	665
85000.0	.27632	600	567	535	503	471	439	407	375	343
86000.0	.27311	279	248	216	184	153	122	90	59	28
87000.0	.26997	966	935	904	873	843	812	782	751	721
88000.0	.26690	660	630	600	569	539	509	480	450	420
89000.0	.26390	361	331	302	272	243	214	184	155	126

Table 3.3 (Cont'd)

	.0	100.0	200.0	300.0	400.0	500.0	600.0	700.0	800.0	900.0
90000.0	.26097	68	39	10	5982	5953	5924	5896	5867	5839
91000.0	.25810	782	754	726	697	669	641	613	585	558
92000.0	.25530	502	474	447	419	392	364	337	310	282
93000.0	.25255	226	201	174	147	120	93	67	40	13
94000.0	.24987	960	934	907	881	854	828	802	776	750
95000.0	.24724	698	672	646	620	594	568	543	517	492
96000.0	.24466	441	415	390	365	339	314	289	264	239
97000.0	.24214	189	164	139	114	90	65	40	16	3991
98000.0	.23967	942	918	894	869	845	821	797	773	749
99000.0	.23725	701	677	653	629	605	582	558	534	511
100000.0	.23487	464	441	417	394	371	347	324	301	278
101000.0	.23255	232	209	186	163	140	118	95	72	49
102000.0	.23027	4	2982	2959	2937	2915	2892	2870	2848	2825
103000.0	.22803	781	759	737	715	693	671	649	628	606
104000.0	.22584	562	541	519	498	476	454	433	412	390
105000.0	.22369	348	326	305	284	263	242	221	200	179
106000.0	.22158	137	116	95	75	54	33	13	1992	1971
107000.0	.21951	930	910	889	869	849	828	808	788	768
108000.0	.21748	727	707	687	667	647	627	608	588	568
109000.0	.21548	528	509	489	469	450	430	411	391	372
110000.0	.21352	333	313	294	275	256	236	217	198	179
111000.0	.21160	141	122	103	84	65	46	27	8	990
112000.0	.20971	952	934	915	896	878	859	841	822	804
113000.0	.20785	767	749	730	712	694	676	657	639	621
114000.0	.20603	585	567	549	531	513	495	477	459	442
115000.0	.20424	406	388	371	353	335	318	300	283	265
116000.0	.20248	230	213	196	178	161	144	126	109	92
117000.0	.20075	58	40	23	6	9989	9972	9955	9938	9921
118000.0	.19905	888	871	854	837	821	804	787	771	754

4.0 Technical Description

4.1 Detector Head

In order to reduce the level of external interference, two identical coils each of inductance 34.9 mH and 6.2 Ω resistance wound from 950 turns of #19 gauge copper wire were arranged anti-parallel to each other and connected via a coaxial cable to the "bottle" input on the magnetometer, in the detector first used with this instrument. Other similar coils have later been used in both single and double coil arrangements. All can be tuned by switches BT1 and BT2. The liquid used inside these coils has always been distilled water of a commercial (battery) grade contained in a 250 cc plastic container.

4.2 Polarization and Removal of the Polarizing Field

During polarization 24 V (12 V sufficient) is applied across the coil via contacts A_{1b} and B_{1b} for 4 secs (Fig. 5). Relay B has a 100 μF capacitor in parallel with it and is fed via a diode and surge limiting resistors of 10 Ω. Since pin (1) of the subchassis S_1 is kept at -12 V, whenever pin (8) is earthed by the polarizing control system both relays A and B operate; however, after removal of the current, relay A opens immediately (the protecting diode across it prevents any spikes) while relay B is delayed approximately 10 milliseconds by virtue of the 100 μF capacitor shunting it.

The 10-millisecond delay between relay A opening and relay B opening is used to quench the current flowing in the bottle. As soon as A_{1b} opens, the voltage across the bottle goes positive forcing the 1N3195 diode to conduct and charging the 60 μF, 50 V capacitor up to approximately 24 V. This voltage causes the current in the bottle to decrease until it eventually goes through zero; the diode cuts off and prevents the 60 μF capacitor from discharging into the bottle. This process takes approximately 3 milliseconds and is used to prevent the formation of large voltage spikes across relay A_{1b} contacts while ensuring a sufficiently rapid removal of the polarizing field. While this process has been occurring, relay B has remained energized and has been earthing the input to the amplifier to protect it via contact B_{2b} and the computing section has been reset by the opening of contact B_{2a}. When relay B opens, the reset line is grounded via B_{2a} and the bottle connected to the amplifier by B_{1a}.

4.3 Amplifier

The amplifier input is tuned and has the following general arrangement shown in Fig. 8. C_1 and C_2 are chosen to resonate with the coil at the highest proton frequency of interest and to provide the correct step-down ratio between the bottle and the transistor at the lowest proton frequency of interest. If R_{ω_1} is the ac series circuit resistance at the lowest proton frequency of interest ω_1 and R_{in} the effective input resistance of the amplifier, then

$$(1/C_2)/\ (1/C_1)+(1/C_2) \quad = \sqrt{R_{in}/\left[(\omega_1^{\,2} L^2)/(R_{\omega_1})\right]}$$

and C_3 is chosen so that

$$\omega^2 L \times (C_3 + \frac{C_1 C_2}{C_1 + C_2}) = 1. \quad \text{(L is bottle inductance.)}$$

C_3 is made up of two switches BT_1 and BT_2 on the front panel, each increasing the capacitance in steps of 0.03 μF and 0.003 μF respectively. Two more transistor stages of amplification follow the low noise input stage and this output is fed to the fine filter via the link between pins B and C on plug P_2. The fine filter is tuned to FT_1, FT_2 and FT_3 and the appropriate settings of these for various counts and the settings of the bottle filter appear in Figs. 1 and 2. The output from the fine filter is fed to a single transistor amplifier S_2 (monitoring point: at pin C on plug P_2), and the signal is again amplified and fed to the pulse shaper PS_1 and via a 22 kΩ level setting resistor to an amplifier in S_3.

4.4 Signal Amplitude Meter

The output of S_3 is used to drive the rectifying circuits in S_{4b} for the meter indication of proton signal amplitude (switched by the FUNCtion switch). For a reliable reading the meter 1 should reach at least 6 on the scale when measuring the proton amplitude.

4.5 Computing Circuits (Fig. 9)

As the frequency of proton precession is to be measured to a high degree of accuracy, the period measurement method has been used. Thus the time taken for 1000 cycles of the proton signal to occur is determined by counting the number of pulses produced from a 100 kHz standard crystal in that time. (A block diagram of the circuit is shown in Fig. 4.)

When the polarizing current in the bottle is removed, a spike is sent through the amplifier which causes the tuned circuit of the fine filter to ring. In order to allow this transient to decay, a delay of 0.2 sec is made before starting the determination of the proton frequency.

4.5a Divider chain and binaries

The units prefixed TS are commercially available transistorized modules manufactured by Venner Electronics, New Malden, Surrey, England.

The 1000 counter is made up of two TS11 units and one slightly modified TS11. When the grey reset line is ungrounded all the computing elements except A_1 are set in the 0 state. A_1 is set by internal adjustments to the wiring to 6 so that the count in the counters stands at 600 after resetting. Thus, after relay B de-energizes, decade counter A_1 will produce its first pulse only after 400/2000 secs = 0.2 sec; the next pulse from counter A_1 will of course occur 1000 proton cycles later. These two pulses control the opening and closing of gate G_1 via the interlock binaries B_1 and B_2. The first pulse alters the state of B_2 and this change is fed from pin 2 of B_2 to pin 4 of B_1 causing it to change its state and the gate G_1 to open; the next pulse changes the state of B_1 via pin 6 of B_1 causing the gate to close. Further pulses will not change the state of the binaries until the binaries are reset. Binary B_1 controls the gate and when the gate, G_1, is open the 100 kHz crystal oscillator pulses are fed into the decade chain.

4.5b Decade chain

This consists of five decade (divide by ten) units. The first unit, C5, is a medium speed unit TS10MF, while the remaining four C units are low speed units TS11LF. The state of the counters is displayed on a set of meters on the front panel.

To allow for individual counter differences, trimming controls for the meters are provided (Fig. 18). To set these correctly the "SET 0" button should be pressed (this breaks the reset line between the C counters and the controlling binaries, thus resetting only the C counters); the 10 kΩ potentiometers are then adjusted so that all the meters read 0. After setting the "ADJUST 9" control on the front panel to its mid-position, the "SET 9" button should be pressed and the 500 Ω potentiometers adjusted so that all the meters indicate 9. The "SET 0" button should be then again pressed and the 10 kΩ potentiometers readjusted if necessary. The 5 Ω "ADJUST 9" control is used to compensate for battery voltage changes during operation and should be adjusted whenever necessary.

Note that current output from the decades $C_1 \longrightarrow C_5$ are passed via plug P_1. This plug normally has links but if automatic readout is desired it is suggested that a recorder be stepped sequentially observing the output currents in each of the decades

4.6 Polarization Control (Fig. 10)

Polarization control is initiated by momentarily connecting the polarization bus to -10 V via the push-button POLARIZE or pins P on the output plugs. The -10 V pulse is converted into a -3 V pulse by a potential divider circuit comprising a 22 kΩ resistor and a 10 kΩ resistor and fed via a diode into the delay timer DT_1. The output at pin (1) is normally at -9 V but once initiated the output falls to -1 V for 5 secs. This time delay is set by a 200 kΩ resistor. The output from pin (1) is fed to pin (6) of the polarizing control sub-unit on chassis S_{4b}. A 3.3 V zener diode prevents the -1 V from passing through the 68 kΩ resistor and the 2N520 transistor is cut off forcing the 2N1305 to saturate and thus the relays A and B connected to pin (1) of chassis S_4 via pin (8) on chassis S_1 to operate. When the delay timer DT1 reverts to resting state after 5 secs, the output (pin 1 on DT1) reverts to -9 V forcing 0.1 mA to flow through the 68 kΩ resistor in S_4 (Fig. 7) and the 2N520 to saturate and the 2N1305 to be cut off. Plugs P_1 and P_2 contain facilities for initiating a polarization sequence by application of a -10 V pulse on pin P.

4.7 Crystal Oscillator (Fig. 9)

The crystal oscillator is contained complete with its amplifier circuits in the TS25 unit. The frequency of the oscillator can be observed on pin M of plug P_1. The crystal should be standardized by placing a suitable capacitor across pins (7) and (8) of OSC plug. This should be between 0 and 100 pF and should be chosen so that the frequency of oscillation is 100 kHz ± 1 Hz.

4.8 Power Supplies (Fig. 11)

The polarizing supply to the bottles is fed directly from pin C of the battery via pin (2) of unit S1. The -12 V supply is used to control the polarizing relays A and B directly via pin (1) of the S1 units. All other units are supplied via the "ADJUST 9" 5 Ω variable resistor which is used to compensate for battery voltage fluctuations.

All the computing elements are decoupled via resistors (chosen so that a 1 V drop appears across them) and 50 μF capacitors. In addition, two 100 μF capacitors shunt the -12 V line and a reverse-biased diode blows the fuse of the 12 V supply if the supply is connected with incorrect polarity.

4.9 Power Consumption

For most purposes a 12 V polarizing supply will be found adequate; the magnetometer then consumes 230 mA on standby and 1.3 A while polarizing.

5.0 Modifications

Several modifications to a unit such as this are possible. Provision has been made on plug 1 for connection to a pen recorder of the count displayed in analogue fashion on the meters of the front panel. The addition of automatic recycling circuits to the unit would then result in an automatic base station recording instrument. The count which is generated in a binary coded decimal form could also be recorded digitally but the particular transistor modules used here are not well suited to drive a digital recorder.

Three modifications to the unit which have applications in marine surveying will be mentioned.

5.1 Deep-Tow Version

The deep-towed instrument package, under development at MPL, is well suited for making magnetic measurements at depth in the oceans. The case of this device can contain the polarizing power, the programming unit, and the preamplifiers for the signal. The output of this amplifier is fed up a cable to the ship where the portable magnetometer is used to amplify the signal, select the signal from the noise in its tuned stage and count the signal's frequency.

A further modification of this device was used in a self-contained package in the search for the submarine THRESHER. This operation made use of 12,000 feet of cable aboard the ship GIBBS and readings were taken every 30 secs during working periods which could extend to twelve hours before the polarizing power had to be replenished. Details of this operation will be available in a separate report (Belshé, in preparation).

5.2 Bathyscaph Version

Again motivated by the search for THRESHER the portable magnetometer was used aboard the bathyscaph TRIESTE. The instrument was contained in the control room and connected through bulkhead pressure connectors to the detector (bottle) which was floated 300 feet above the vehicle. Polarizing power and programming circuits (manual, at-command, interrogation was actually used) could also be contained within the hull, but electrical interference required a preamplifier to raise the signal level before it came through the bulkhead connectors. Such an amplifier was housed in a small high-pressure case on the upper deck of the TRIESTE. A complete description of this system is also in the THRESHER report.

5.3 Gradiometer Version

The layout of the module base connections has been made in a way which will permit easy modification of the magnetometer to a differential form following measuring procedures we have developed (Mudie, 1963). This would require certain additional counting units and an external amplifier for the second signal channel.

REFERENCES

Abragam, A. (1961): The Principles of Nuclear Magnetism, Oxford University Press.

Aitken, M. J. (1961): Physics and Archaeology (Interscience Publishers, New York.

Bloch, F. (1946): Phys. Rev., 70, 461.

Hill, M. N. (1959): Deep Sea Research, 5, 309-311.

Mudie, J. D. (1963): Archaeometry, 5, 135-138.

Packard, M. and R. Varian (1954): Phys. Rev., 93, 941.

Schiff, L. I. (1955): Quantum Mechanics, McGraw Hill, New York.

Varian Associates: Portable magnetometer data sheet, M-49A, Palo Alto, California, U.S.A.

Vigoureux, P. (1963): Nature, 198, 488, 1188.

Warren, R. E. and V. Vacquier (1961): A ship-towed proton magnetometer, MPL Technical Memorandum No. 120.

Waters, G. S. and P. D. Francis (1958): J. Sci. Instr., 35, 88-93.

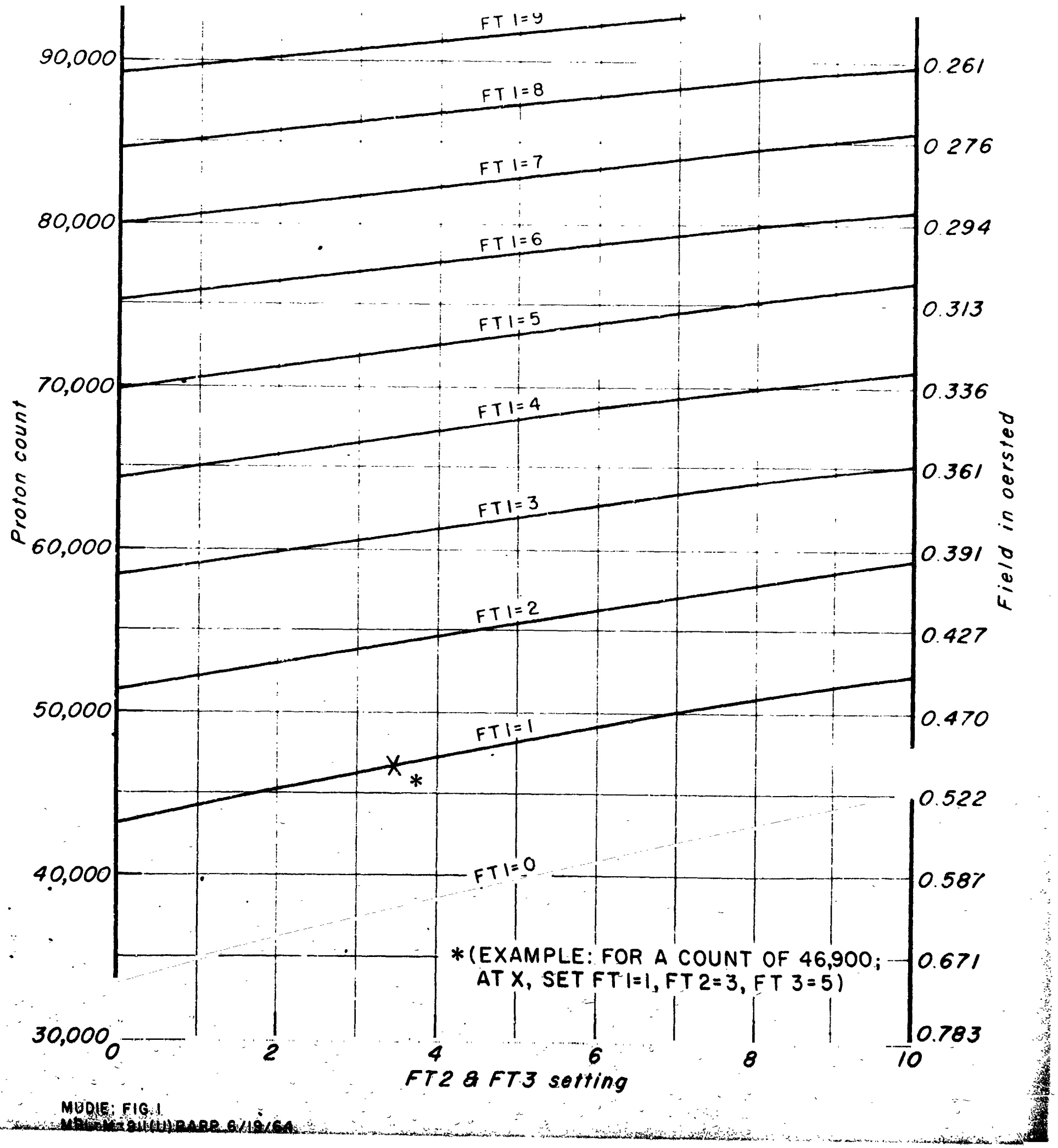

MUDIE: FIG. 1
MDL-M-911(U) PARP 6/19/64

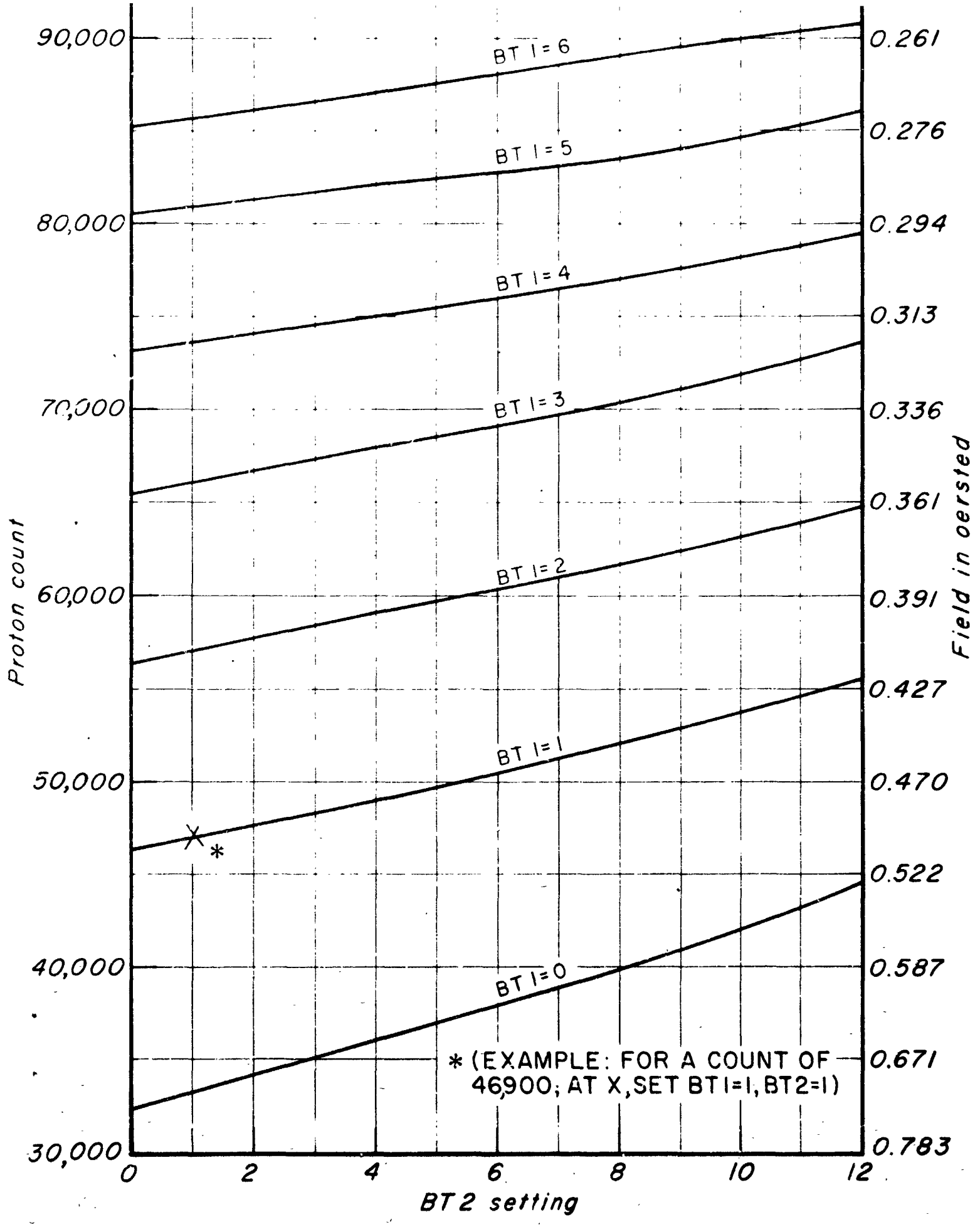

MUDIE: FIG. 2
MPL-M-912 (U) / RAPP 6/19/64

OVERSIZED

INCLUSIONS

NOT

FILMED

REQUEST

FROM

ORIGINATOR

SCHEMATIC LAYOUT

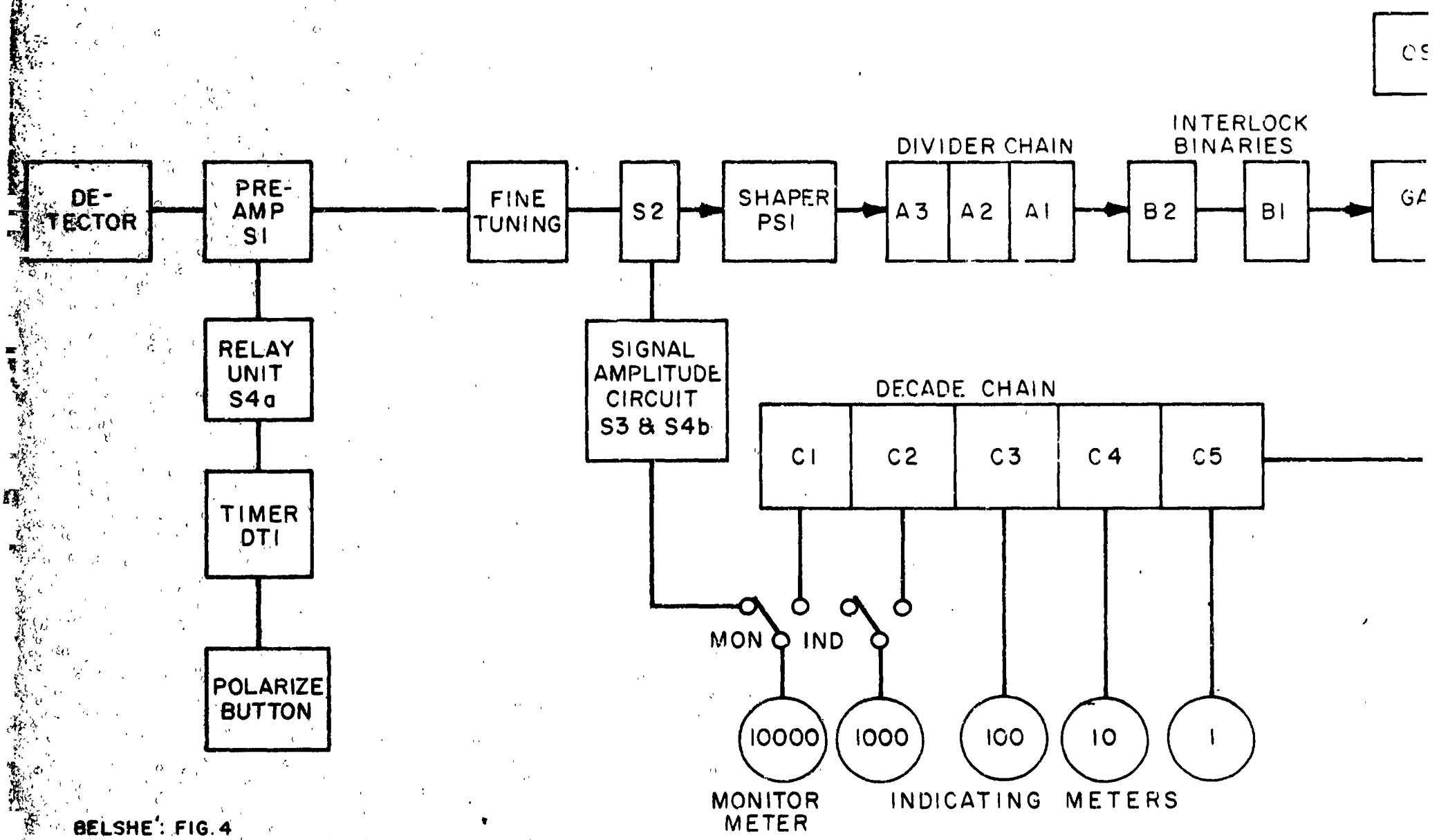

BELSHE': FIG. 4
MPL-M-873(U)/RAPP 3/18/64

PORTABLE PROTON MAGNETOMETER PREAMPLIFIER S/B

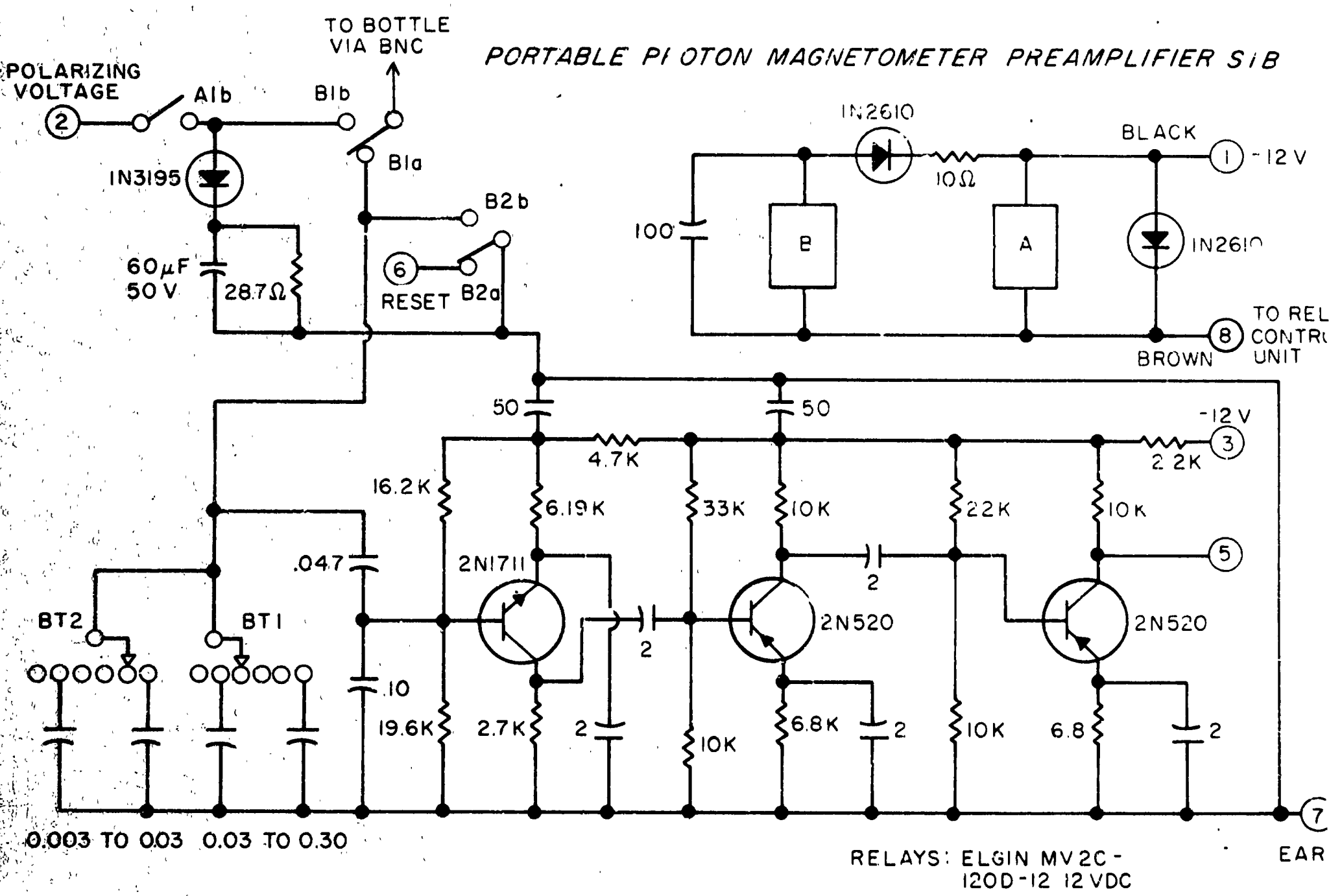

BELSHE': FIG. 5
MPL-M-874 (U)/RAPP 3/23/64

SIGNAL PRODUCTION CIRCUITS

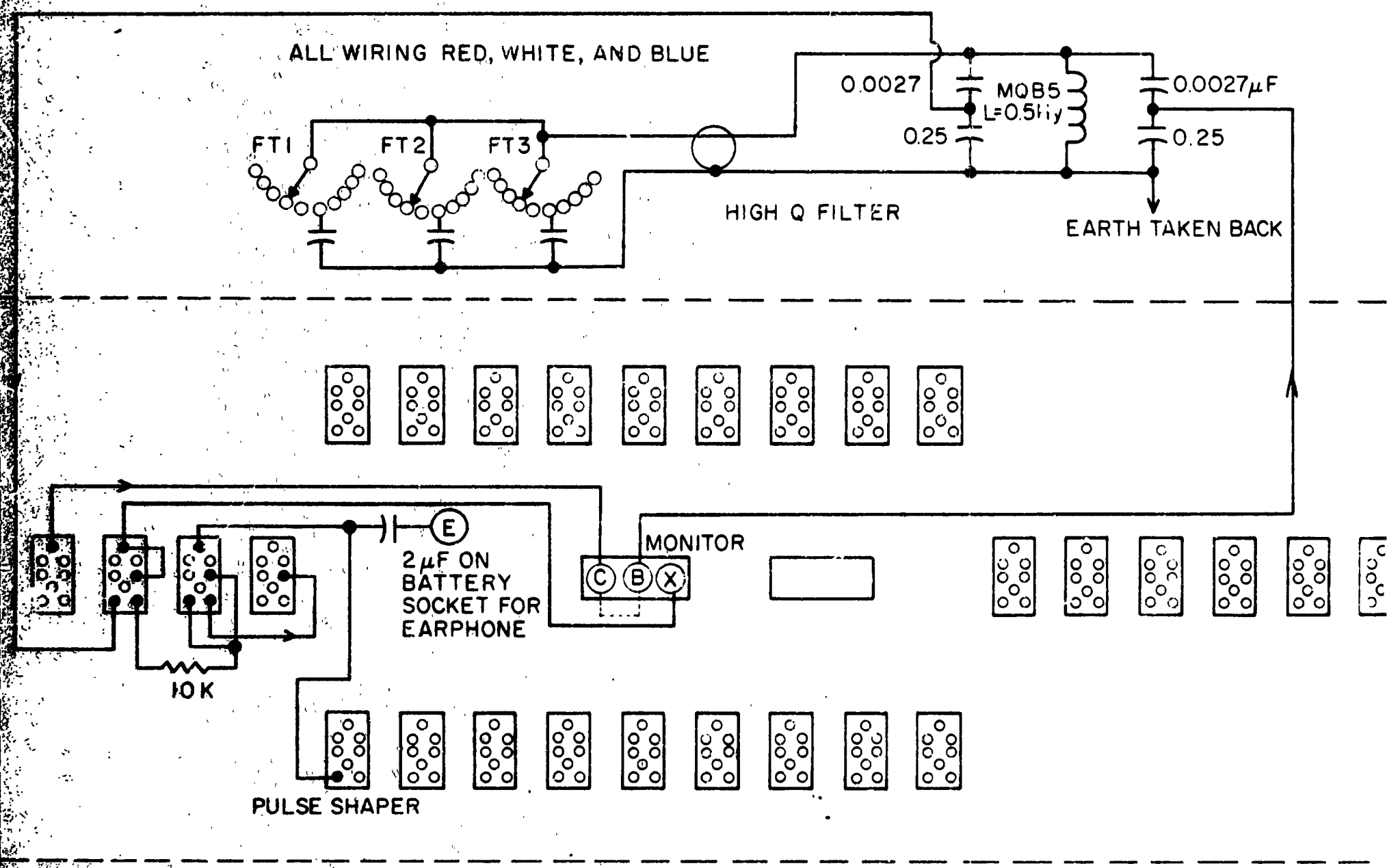

BELSHE': FIG. 6
APL-M-875(U)/RAPP 3/23/64

SUB CHASSIS S4

(a)

(b)

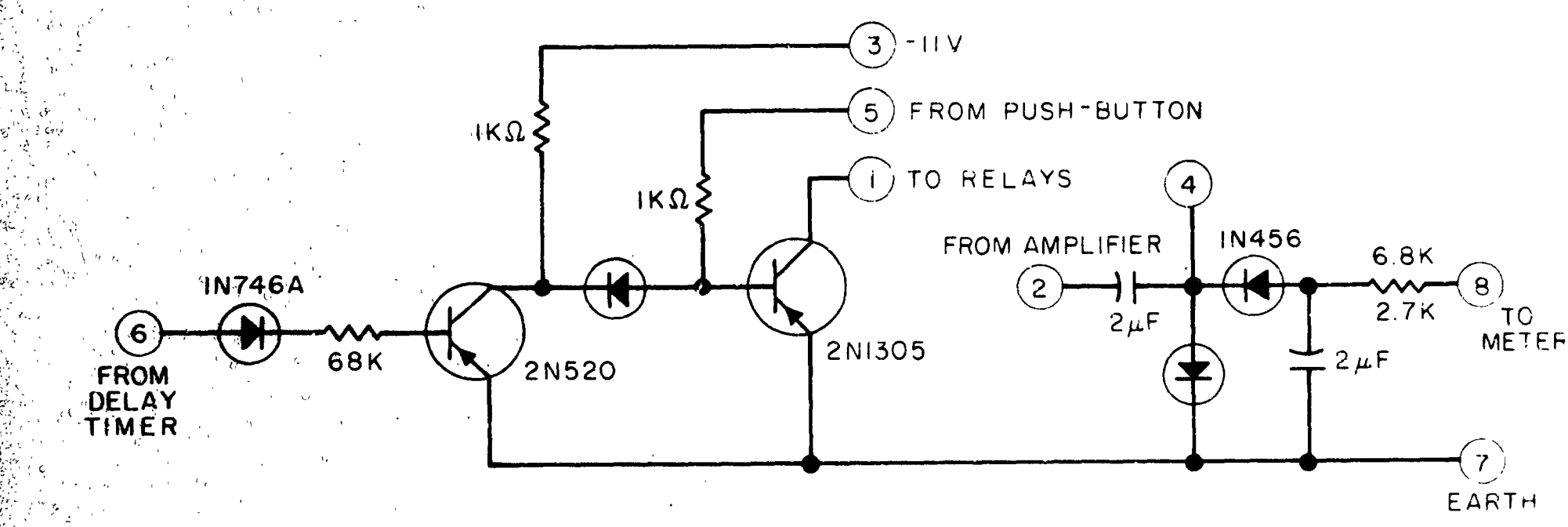

BELSHE: FIG: 7
MPL-M-876(U)/RAPP 3/23/64

INPUT MATCHING SCHEMATIC

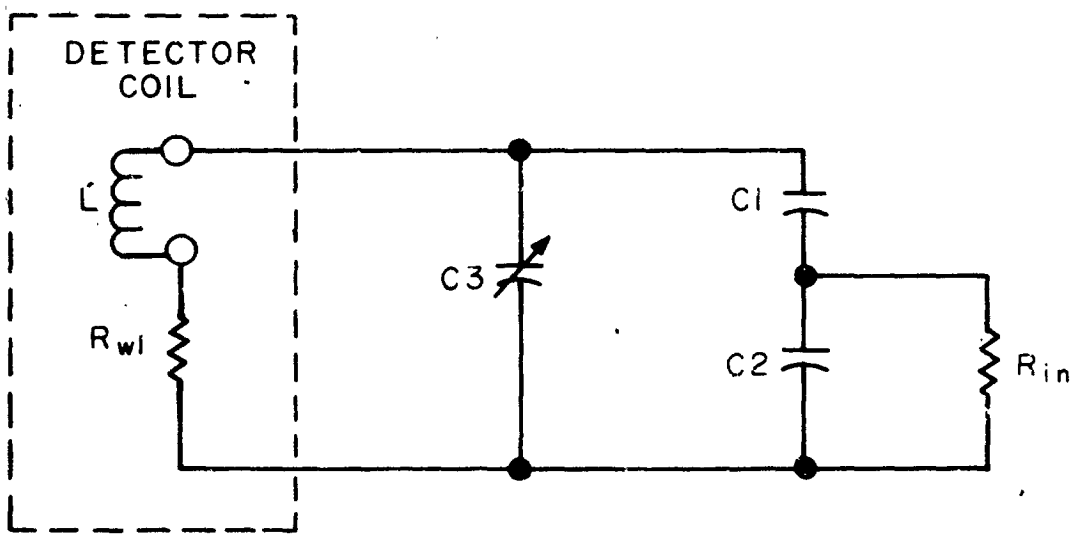

BELSHE: FIG.8
MPL-M-877 (U)/RAPP 3/23/64

COMPUTING WIRING OF MAGNETOMETER

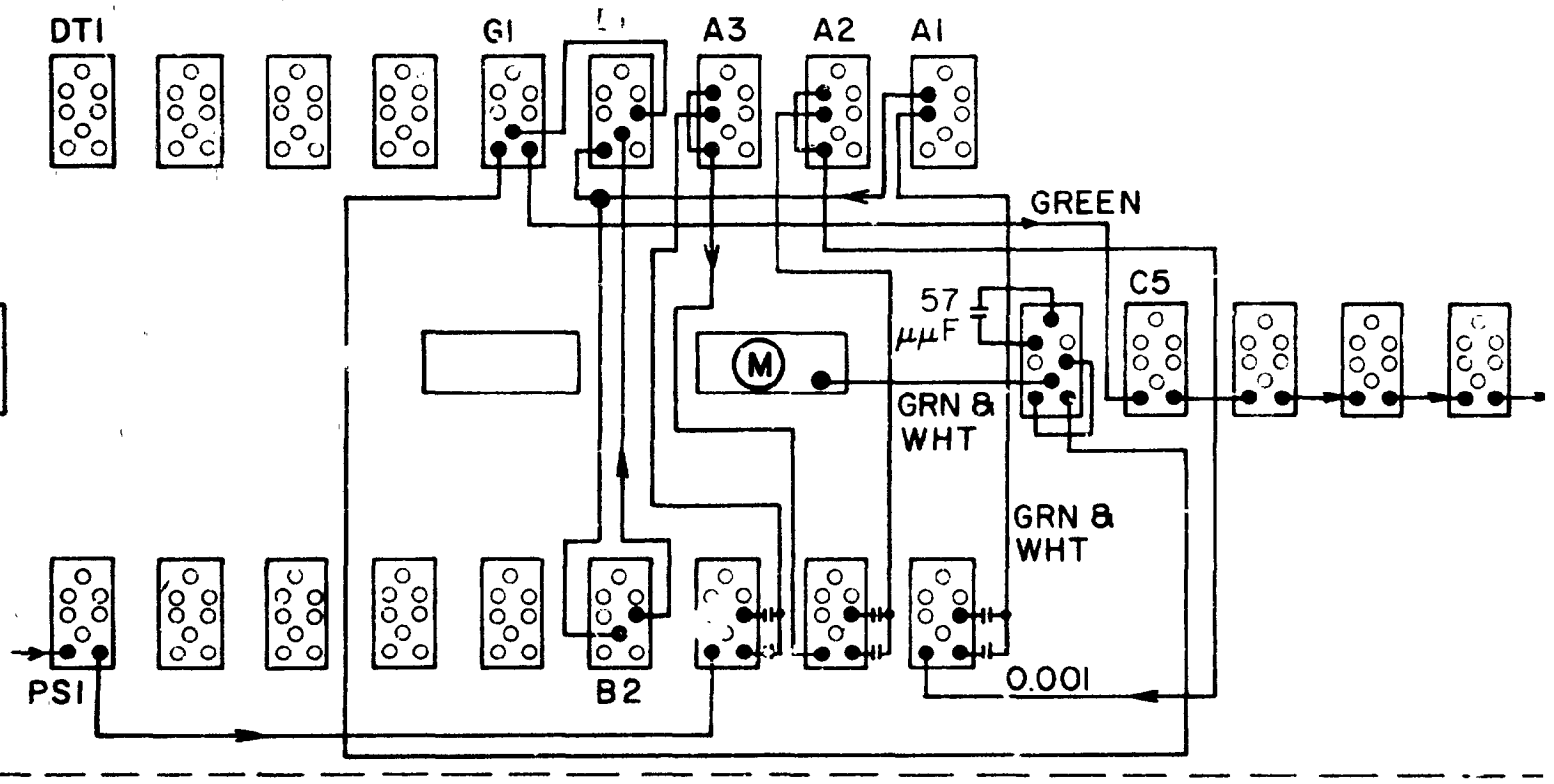

BELSHE': FIG. 9
MPL-M-878(U)/RAPP 3/23/64

POLARIZATION CONTROL AND RESET LINES

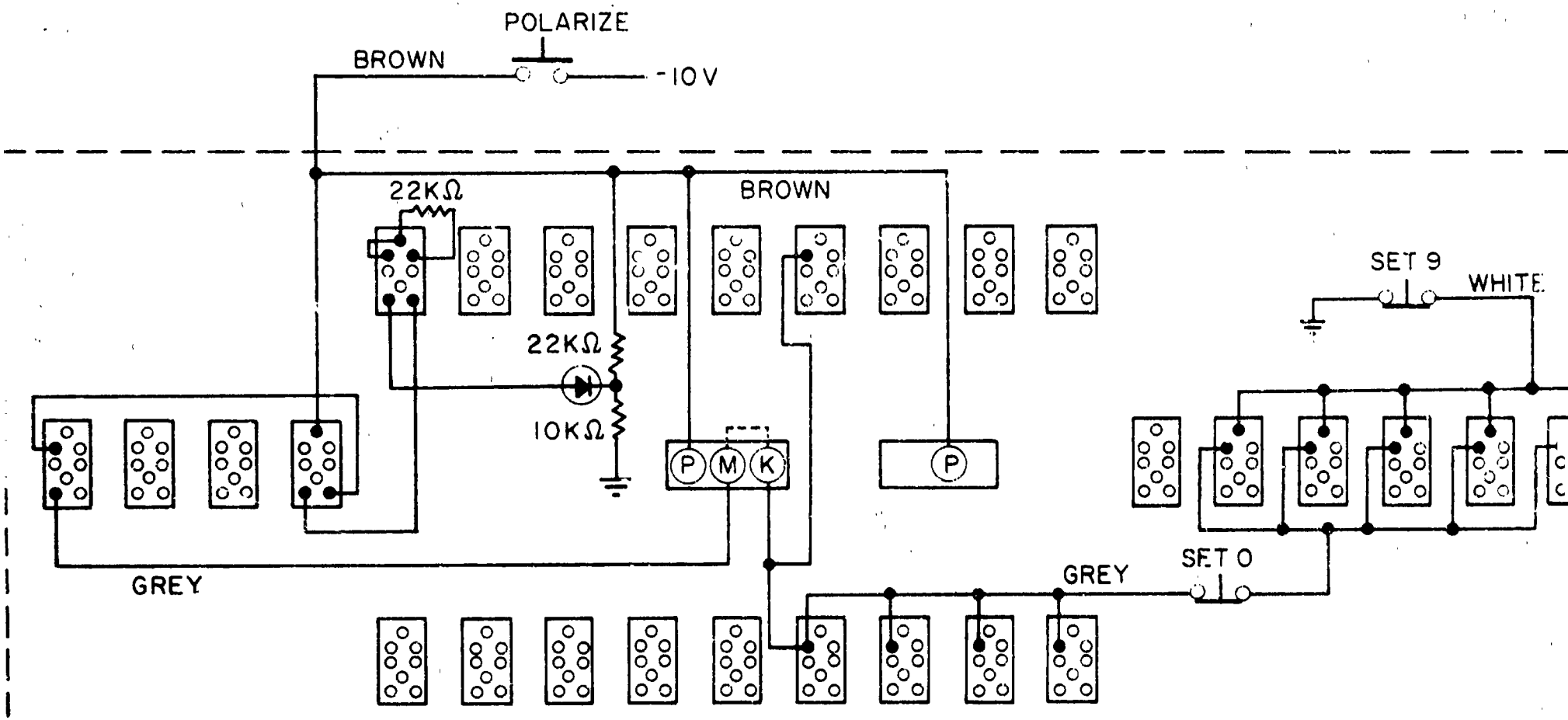

POWER SUPPLY WIRING OF MAGNETOMETER

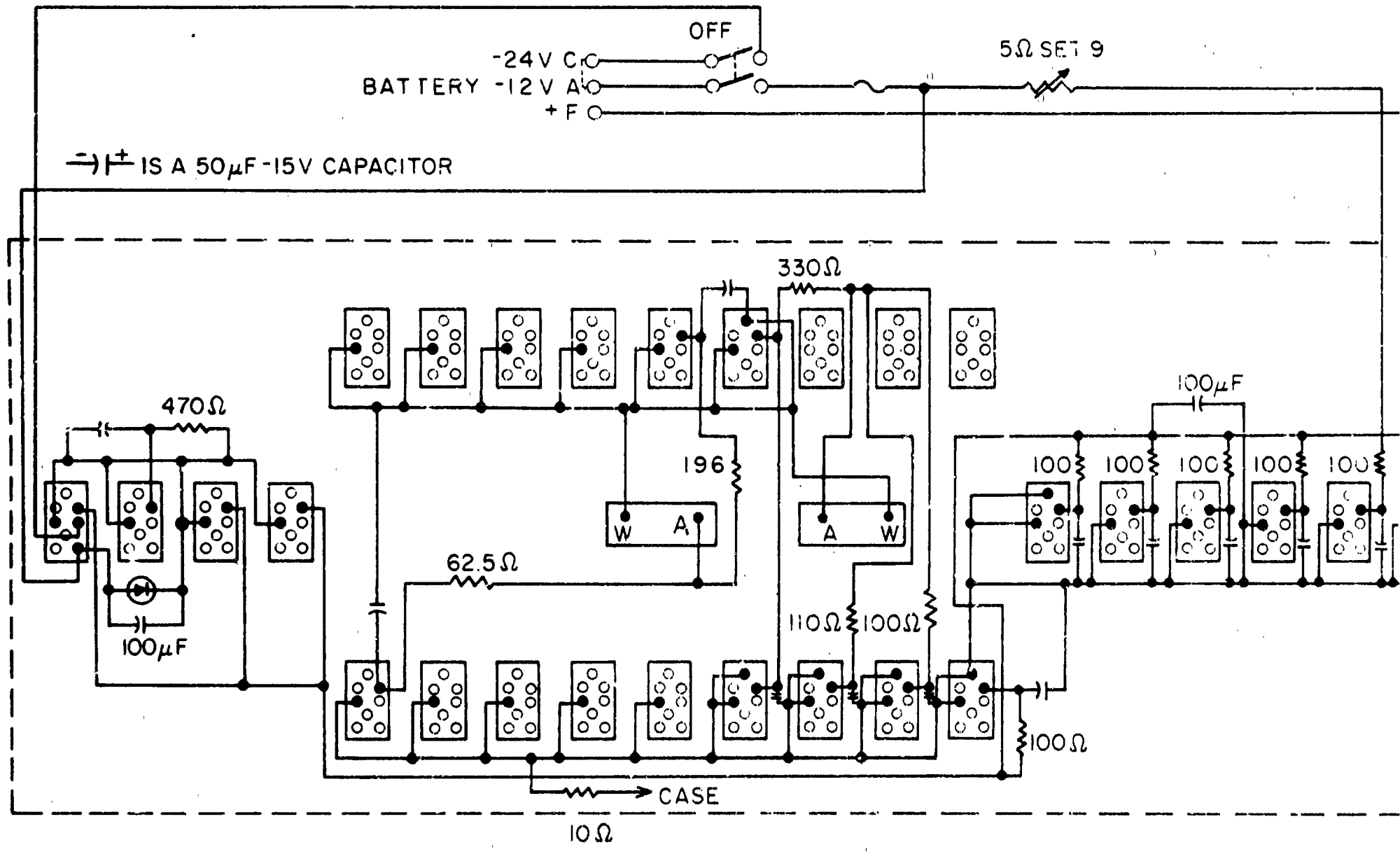

BELSHE'; FIG. 11

LOCATION OF UNITS

S1	SPECIAL UNIT	B1 & B2	VENNER TS2B
S2 & S3	VENNER TS4	A2 & A3	VENNER TS11
S4	SPECIAL UNIT	A1	VENNER TS11 MODIFIED
PS	VENNER TS 14	OSC	VENNER TS25 WITH 100 K c/s CRYSTAL
DT1	VENNER TS 18	C5	VENNER TS10/MF
G1	VENNER TS 16	C1,C2, C3, & C4	VENNER TS10/LF

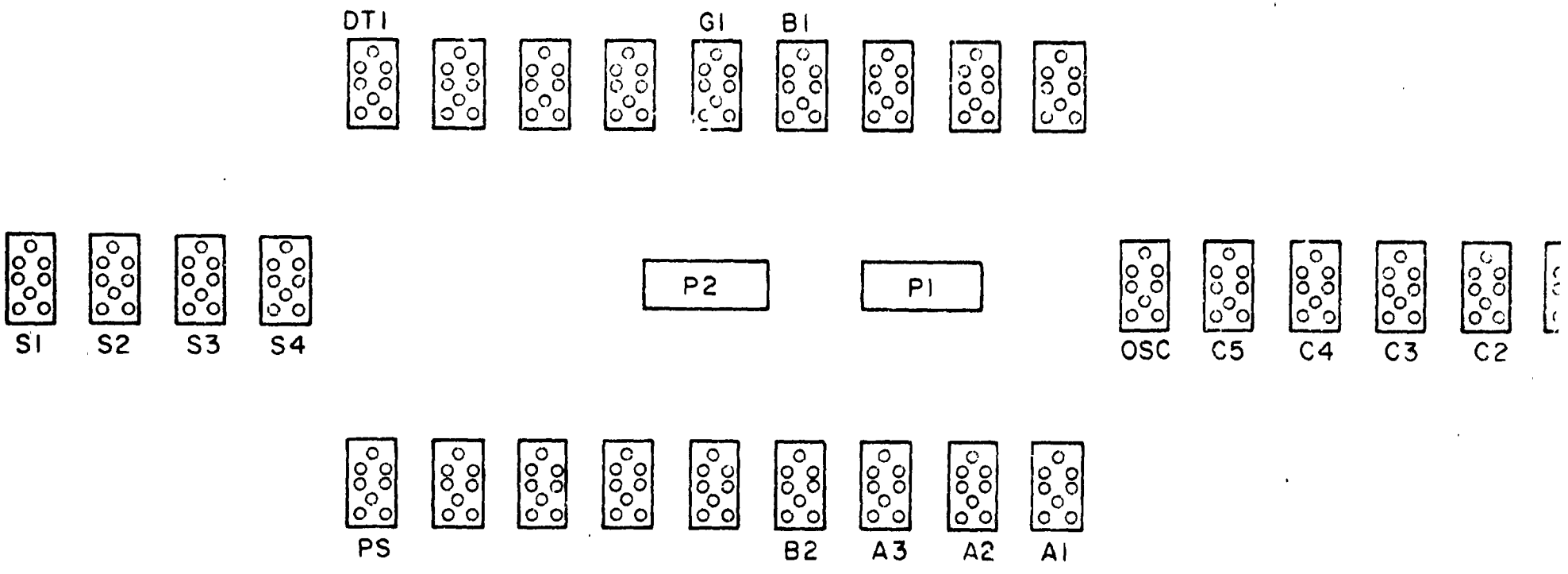

C1 & C2 ARE WIRED IN A SIMILAR FASHION C3, C4, & C5 DO NOT HAVE THE MON, IND SWITCH

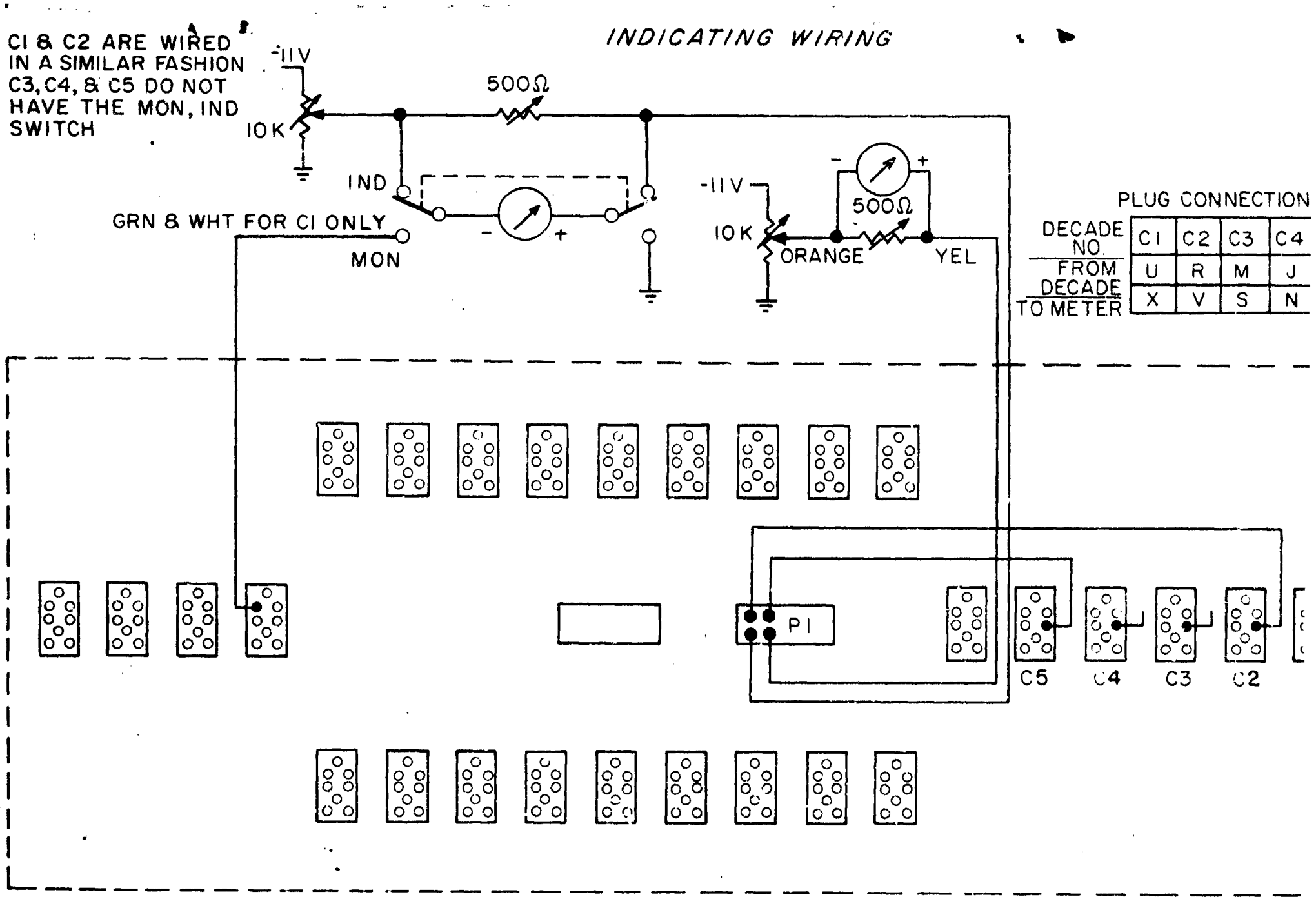

PLUG CONNECTION

DECADE NO.	C1	C2	C3	C4
FROM DECADE	U	R	M	J
TO METER	X	V	S	N